Available online at www.sciencedirect.com

ScienceDirect

Energy Procedia 124 (2017) 799–805

Energy Procedia

www.elsevier.com/locate/procedia

7th International Conference on Silicon Photovoltaics, SiliconPV 2017

Two-stage permanent deactivation of the boron-oxygen-related recombination center in crystalline silicon

Verena Steckenreiter[a,]*, Dominic C. Walter[a], Jan Schmidt[a,b]

[a]*Institute for Solar Energy Research Hamelin (ISFH), Am Ohrberg 1, D-31860 Emmerthal, Germany*
[b]*Department of Solar Energy, Institute of Solid-State Physics, Leibniz Universität Hannover, Appelstraße 2, D-30607 Hannover, Germany*

Abstract

We analyze the lifetime evolution during permanent deactivation of the boron-oxygen-related defect center (BO defect) in boron-doped, oxygen-rich Czochralski-grown silicon (Cz-Si). In particular, we examine the impact of the samples' states prior to the permanent deactivation process. Samples that were initially fully degraded show a two-stage deactivation process consisting of a fast and a slow deactivation component, which can be fitted by two exponential functions with their respective rate constants. For both components, we find a pronounced increase of the rate constants with illumination intensity. In addition, we observe that the rate constant describing the slow deactivation component of samples deactivated after complete degradation is identical to the rate constant determined on samples, which were deactivated immediately after annealing in darkness. In the latter case, a purely mono-exponential deactivation behavior was observed. Our study clearly demonstrates that the asymptotic deactivation behavior does not depend on the initial state of the lifetime sample. We prove that the same is valid for initially degraded and dark-annealed PERC solar cells. Hence, it is not necessary to first degrade the sample to realize a fast BO deactivation.

Peer review by the scientific conference committee of SiliconPV 2017 under responsibility of PSE AG.

Keywords: boron-oxygen defect; Czochralski silicon; permanent deactivation; carrier lifetime

1. Introduction

Light-induced degradation (LID) affects the solar cell's power output by limiting the bulk carrier lifetime [1]. LID occurs in presence of boron and oxygen in crystalline silicon, both species being typically present in boron-

* Corresponding author. Tel.: +49-5151-999-325; fax: +49-5151-999-400.
E-mail address: v.steckenreiter@isfh.de

1876-6102
Peer review by the scientific conference committee of SiliconPV 2017 under responsibility of PSE AG.
10.1016/j.egypro.2017.09.350

doped Czochralski-grown silicon (Cz-Si) [2,3]. For now more than 10 years, a procedure is known that permanently reverses the lifetime degradation due to recombination-active BO defect centers [4]. In this procedure, the lifetime degradation is permanently reversed by illumination at elevated temperature, a process referred to as 'permanent deactivation' of the BO defect or 'regeneration' of the lifetime or solar cell efficiency [4]. The impact of the temperature during permanent deactivation on the deactivation rate constant R_{de} follows an Arrhenius law [5,6]. Furthermore, R_{de} depends directly on the excess carrier density Δn manipulated by the chosen illumination intensity as recently shown [5,7–9]. Additionally, it has been conjectured that the deactivation kinetics of BO center depends on the samples's pre-history [10–12]. However, this has not been examined in detail so far.

In this contribution, we analyze the influence of the initial state of the Cz-Si samples on the lifetime evolution during the deactivation process. We observe a strictly mono-exponential decay of the effective defect concentration N_t* in case of initially dark-annealed samples, in agreement with reports in the literature [13]. In contrast, initially fully degraded samples show a two-stage deactivation process with a fast component in the very beginning and a slower component of comparable magnitude as from dark-annealed samples. Furthermore, we confirm the discovered two-stage deactivation on the solar cell level. This finding leads to the conclusion that the initial degradation reveals a second deactivation mechanism. However, this fast component does not lead to a faster deactivation of the defect center in general.

2. Experimental details

We use commercially available boron-doped Czochralski-grown silicon (Cz-Si) wafers with resistivities of 1.0 Ωcm (i.e. p_0=1.5 × 10^{16} cm^{-3}) and 2.2 Ωcm (i.e. p_0=6.5 × 10^{15} cm^{-3}), respectively. The wafers are processed into lifetime samples at full size of 156×156 mm^2. After saw-damage removal in KOH and a standard RCA-cleaning [14] sequence, a phosphorus diffusion is performed resulting in an n^+-region with a nominal sheet resistance of ~100 Ω/sq. Subsequently, the PSG is removed using HF and the n^+-region is removed from several samples using KOH. The sample thickness is ~150 µm in case of the 1.0 Ωcm samples and ~136 µm for the 2.2 Ωcm samples. All samples pass through an additional RCA cleaning before receiving a 10-nm thick Al_2O_3 layer deposited via plasma-assisted atomic layer deposition (plasma ALD) [15]. Subsequently, we deposit a 70-nm-thick SiN_x capping layer on top (refractive index n = 2.05 at λ = 632 nm) via plasma-enhanced chemical vapor deposition (PECVD). Now all samples undergo a rapid thermal annealing (RTA) step in a commercial belt-line furnace (DO-FF-8.600–300, centrotherm) at a set peak temperature of 850°C, in order to accelerate the following permanent deactivation process and to introduce hydrogen from the dielectric layers into the silicon bulk [13,16]. After the RTA/firing treatment the wafers are laser-diced into samples of 5 × 5 cm^2.

We analyze the process of permanent BO deactivation starting from two different initial states: (i) the dark-annealed state, and (ii) the fully degraded state. We extract the following characteristic lifetimes:

- τ_0 after annealing in the dark for 10 min at 200°C. This type of BO deactivation is non-permanent and lifetime drops again under illumination. The annealed state does not correspond to a stable defect configuration [1]. Please note, due to the sensitivity of this lifetime state on illumination, this lifetime is afflicted with the highest uncertainty.
- τ_d after degradation due to complete LID. For degradation we illuminate the samples for 38 h at a light intensity of 10 mW/cm^2 at room temperature [17], which results in the maximum concentration of recombination-active BO centers.
- τ_{0p} after complete permanent deactivation. This lifetime is the maximum value measured during the deactivation process.

We systematically vary the light intensity of the halogen lamp used for the deactivation process between 0.5 and 3 suns, usually in steps of 0.5 suns. The measurement uncertainty of the light intensity is within 2 %. During deactivation the samples are placed on a hot plate. To realize steady-state conditions that fit all light intensities, we choose a deactivation temperature of (169.5±3.5)°C for all samples. The lifetime $\tau(t)$ is monitored during the

deactivation process by measuring the lifetime using a Sinton Lifetime Tester WCT-120 (Sinton Instruments) in photoconductance decay (PCD) mode [18] at about 31°C. We extract τ at a fixed injection level of $\Delta n/p_0$=0.1 with Δn being the excess carrier density and p_0 being the equilibrium hole concentration. The BO deactivation correlates with a change in the effective defect concentration N_t* which we determine from the measured lifetime using the equation $N_t^* = 1/\tau(t)-1/\tau_0$.

3. Impact of the initial state on the deactivation of lifetime samples

When starting the deactivation procedure from the dark-annealed state, at least two mechanisms interfere with each other: on the one hand, degradation occurs due to LID since BO centers are activated. On the other hand, due to illumination at elevated temperature recombination-active BO centers are already deactivated. Vice versa, if the initial state is fully degraded, the illumination at elevated temperature reveals the pure permanent deactivation process. Figure 1(a) shows N_t* versus the deactivation time t of two samples deactivated at 1 sun and 170°C. Hereby, the circles show the lifetime evolution of an initially dark-annealed sample and the diamonds of an initially fully degraded sample. The initial lifetime of the annealed sample is with τ_{eff} > 1 ms as high as after permanent deactivation. Although N_t* of the fully degraded sample is higher at the beginning (not shown in Fig. 1(a)), it decreases initially faster than the dark-annealed sample. However, after 100s of deactivation treatment, N_t* of both samples is identical. We conclude that there exist at least two components during deactivation from the fully degraded state: a fast and a slow component. Since defect evolution cannot be described by a mono-exponential decay function, we fit $N_t^*(t)$ by a double-exponential decay function of the form $A \times \exp(-R_{de,fast} \times t) + B \times \exp(-R_{de,slow} \times t) + C$ with the deactivation rate constants $R_{de,fast}$ for the fast stage and $R_{de,slow}$ for the slow stage.

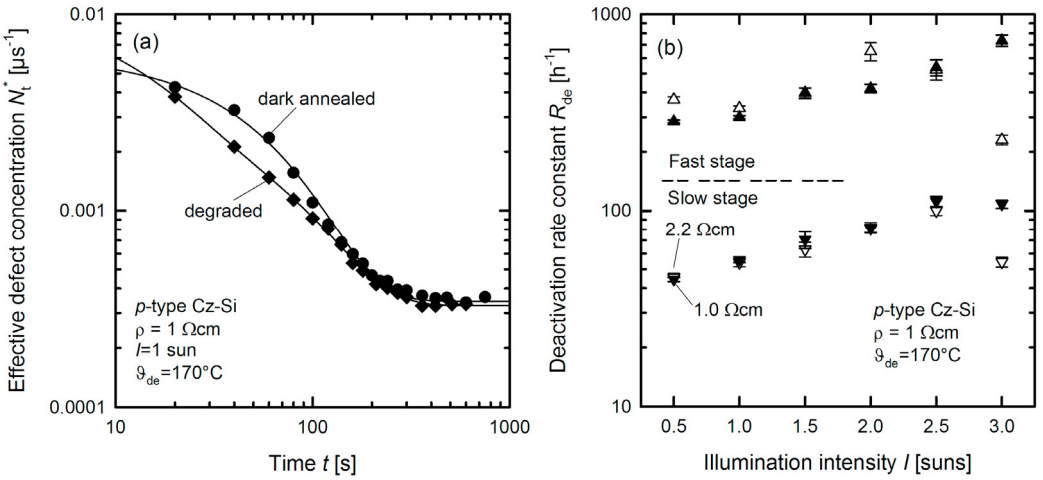

Fig. 1. (a) Effective defect concentration N_t* versus the deactivation time t at an illumination intensity I = 1 sun. Circles symbolize N_t* of the initially dark-annealed sample, diamonds of the initially fully degraded sample. The black lines represent the fits of each curve by a mono-exponential decay (circles) or a double-exponential decay (diamonds) function, respectively. (b) Deactivation rate constants of the slow deactivation stage $R_{de,slow}$ (triangles down) and of the fast deactivation stage $R_{de,fast}$ (triangles up) as a function of the illumination intensity I from initially degraded samples fired at 850°C (set peak temperature) after emitter-removal. Open symbols show the data of the 2.2-Ωcm Si, filled symbols of the 1.0-Ωcm Si samples.

Figure 1(b) displays $R_{de,fast}$ and $R_{de,slow}$ of both examined Cz-Si materials versus the illumination intensity I. For the 1.0-Ωcm Si samples, the deactivation rate constants of the fast deactivation stage $R_{de,fast}$ increases from $(285\pm5)h^{-1}$ at 0.5 suns to a maximum determined value of $R_{de,fast}=(737\pm48)h^{-1}$ at 3 suns. The deactivation rate of the slow stage of the 1.0-Ωcm Si samples increases from $R_{de,slow}=(44\pm1)h^{-1}$ at 0.5 suns to $R_{de,slow}$ =(112±7) h^{-1} at 2.5

suns. Above 2.5 suns the slow deactivation seems to saturate at (108±5) h^{-1}. For the 2.2-Ωcm Si samples the trend of $R_{de,fast}$ and $R_{de,slow}$ versus the illumination intensity is less clear: for example is $R_{de,fast}$=(368±13) h^{-1} at 0.5 suns slightly above the corresponding value at 1 sun. The highest $R_{de,fast}$ is achieved at 2.0 suns with (649±68) h^{-1}, while at I=3.0 suns $R_{de,fast}$ and $R_{de,slow}$ drop significantly to values of (230±13) h^{-1} and (54±3) h^{-1}, respectively. We assume that this drop in R_{de} is not related to the actual illumination-dependent BO deactivation and consider it an outlier. On the other hand, $R_{de,slow}$ determined from the 2.2-Ωcm Si samples is in the range of 0.5 to 2.5 suns of the same magnitude as $R_{de,slow}$ of the 1.0-Ωcm samples with $R_{de,slow}$=(45.±2) h^{-1} at 0.5 suns. The highest $R_{de,slow}$ value is in contrast to the fast component determined at I=2.5 suns with a maximum value of $R_{de,slow}$=(100±5) h^{-1}. The reason for the apparent saturation of the deactivation rate at high illumination intensities can be found in the proportionality of the deactivation rate constant and the excess carrier density R_{de}~Δn [8,9]. Due to the marginal increase of Δn at high illumination intensities, R_{de} seems to saturate as we previously observed at lifetime samples comparable to the ones used in the present study.

Assuming that the slow deactivation is the same mechanism in dark-annealed as well as in degraded samples, we would expect equal values for the deactivation rate constants in case of initially dark-annealed and initially fully degraded samples. Figure 2 shows $R_{de,slow}$ of the degraded 1.0-Ωcm samples (grey triangles) and R_{de} of the initially annealed 1.0-Ωcm samples (black circles) versus I. Although $R_{de,slow}$ increases slightly less pronounced with the illumination intensity than R_{de} of the dark-annealed samples, we indeed observe quite similar values. This supports the assumption of the same physical mechanism responsible for the slow-stage deactivation, independent of the initial state of the sample. Up to now, we can only speculate about the exact physical mechanisms involved regarding the fast component, however, from the degradation process a fast and a slow degradation stage are already known [19], which might correlate to the behavior reported in this study for the permanent deactivation process.

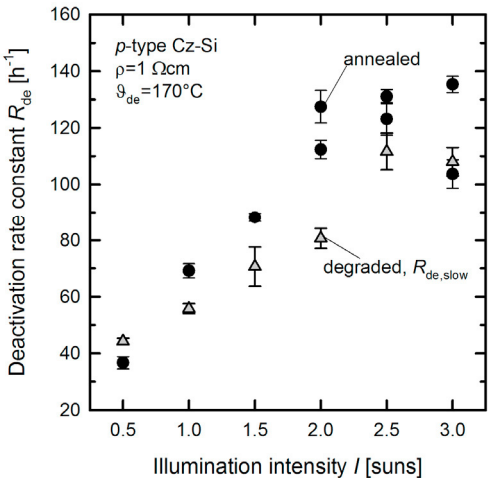

Fig. 2. Deactivation rate constants R_{de} of initially annealed samples (black circles) and $R_{de,slow}$ of degraded samples (grey triangles) versus illumination intensity I.

4. Impact of the initial state on the deactivation of solar cells

The permanent deactivation of the recombination-active BO-defect center in boron-doped, oxygen-rich Cz-Si is of great interest to avoid LID in solar cells. We use the same deactivation treatment as applied before to lifetime samples now for silicon solar cells. For reasons of comparability, we include passivated emitter and rear (PERC) solar cells that are processed from the same 2.2-Ωcm Cz-Si wafer material [20] as used for the deactivation study presented above. The evaluated PERC solar cells are half 6-in PERC cells [21] with a 4-busbar-design optimized for

module-integration; the process-flow is described elsewhere [20]. The solar cells receive a screen-printing metallization and after firing, they are laser diced into half-cells.

We degrade the PERC solar cells by illumination at room temperature for 92 h at an illumination intensity of 10 mW/cm^2 [17]. Subsequently, we deactivate the BO complexes of both half-cells diced from the same initial cell: one half-cell from the degraded state, the other half-cell is non-permanently deactivated by annealing for 10 min at 200°C in the dark prior to applying the deactivation procedure. The deactivation process of the solar cells is carried out just as of the lifetime samples: the samples are placed on a hot plate and the sample temperature is determined to (169.6±0.9)°C. We vary the illumination intensity between 0.5 and 2.5 suns. During the deactivation process, we measure the solar cell parameters using the LOANA solar cell analysis system (pv-tools).

Figures 3(a) and (b) show the evolution of the open-circuit voltage V_{oc} and of the solar cell energy conversion efficiency η during deactivation over time. As observed on the lifetime samples, in case of the initially dark-annealed half-cell (black symbols), two mechanisms compete with each other: since degradation due to LID dominates over the deactivation initialized by illumination at elevated temperature happening at the same time, at the very beginning of the deactivation process there is a drop of V_{oc} followed by the slow deactivation, when the deactivation process starts do dominate. The maximum 'drop' in V_{oc} is in this case less than 2 mV. The V_{oc} of the initially degraded cell is 7 mV reduced at the beginning of the deactivation process, and increases in only 10 s of illumination at elevated temperature by about 3.5 mV, more than the total boost of the dark-annealed half-cell. After the fast-stage increase of V_{oc}, the further deactivation proceeds at slow stage. The solar cell's energy conversion efficiency η develops according to the evolution of V_{oc} during the deactivation process. When the solar cell is initially dark-annealed, a small drop in η is observed by about 0.2 % absolute. It reaches its minimum after 45 s of illumination at elevated temperature, just when V_{oc} reaches the minimum. That the solar cell efficiency does not reach the initial level again despite the successful regeneration of V_{oc} seems to be induced by other, not BO-related effects. On the initially degraded half-cell we observe an evolution with a significant increase at the very beginning of the deactivation procedure and subsequent, slower deactivation, comparable to the trend of V_{oc} during the deactivation. This half-cell reaches a slightly higher η than the dark-annealed one. Finally, an efficiency increase of 0.65 % absolute is achieved due to the deactivation of the BO center compared to the fully degraded state.

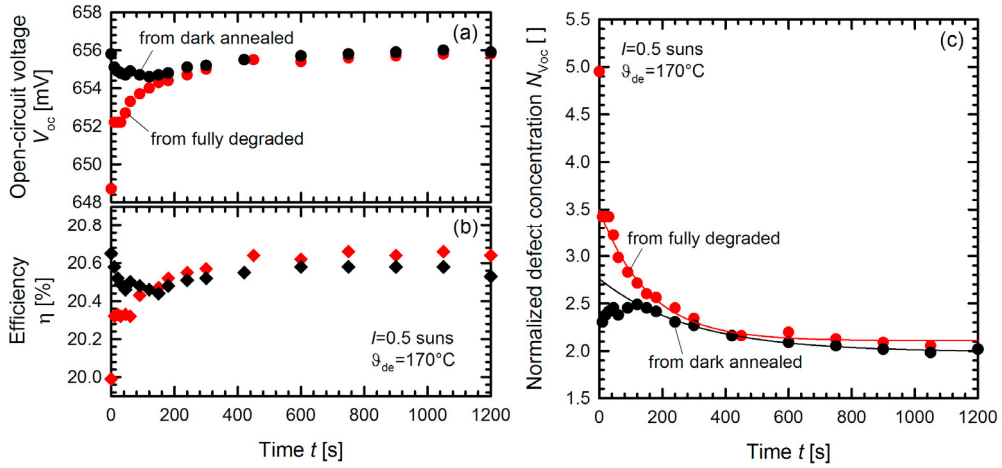

Fig. 3. Evolution of (a) open-circuit voltage V_{oc},(b) solar cell energy conversion efficiency η during deactivation over time and (c) normalized defect concentration N_{Voc}. Black symbols show the development of a solar cell deactivated from the dark-annealed initial state, red symbols from the fully degraded initial state. The deactivation is carried out at 170°C and 0.5 suns. The lines in (c) describe the mono-exponential decay of $N_{Voc}(t)$.

From the time-dependent open-circuit voltage measurements one can determine changes of the normalized defect concentration $N_{\mathrm{Voc}}(t)$. According to Bothe [19] the normalized defect concentration is defined as

$$N_{Voc}(t) \equiv \frac{1}{\exp(\frac{qV_{OC}(t)}{nk_BT})} - \frac{1}{\exp(\frac{qV_{OC}(t=0)}{nk_BT})},$$

with q being the elementary charge, n the local ideality factor (here assumed as 1 [22]), k_{B} the Boltzmann constant and T the absolute temperature. As can be seen from Fig 3(c), the normalized defect density $N_{\mathrm{Voc}}(t)$ follows in the later part a mono-exponential decay function. If the solar cell is initially dark-annealed, N_{Voc} (t) can be described by a mono-exponential decay as soon as the deactivation dominates the degradation. In the case when the solar cell has been initially degraded, a mono-exponential decay function describes the evolution of $N_{\mathrm{Voc}}(t)$ after the first measurement. As from the initially degraded lifetime samples, we find a fast-stage component at the very beginning of the deactivation process. However, as only the first data point reveals the fast component, the explicit determination of a fast and a slow deactivation rate is not possible from these measurements. We observe this characteristic development of $N_{\mathrm{Voc}}(t)$ for all chosen illumination intensities.

5. Conclusions

We observed for the first time that the permanent BO deactivation process proceeds within two stages if the deactivation is performed on initially fully degraded Cz-Si lifetime samples. A fast deactivation stage is followed by a slower deactivation stage. The rates of both stages show a pronounced increase with illumination intensity. The slow deactivation component features the same deactivation rate constant on samples, which were initially fully degraded and on those which were annealed in darkness prior to the deactivation process. Our study shows hence that the asymptotic deactivation behavior does not depend on the initial state of the sample.

Solar cells also reveal a two-stage deactivation in case they are initially fully degraded. Due to the conciseness of the observable fast component, hitherto a sole qualitative description is possible. Hence, contrary to previous studies [10–12] our work leads to the conclusion that it is not necessary to first degrade the samples to realize a fast BO deactivation. In fact, it is rather necessary to analyze the slow deactivation process than the fast deactivation, as the slow process limits the time necessary for completing the BO deactivation.

Acknowledgements

The authors thank Cornelia Marquardt for sample processing and Nadine Wehmeier and Dennis Bredemeier for fruitful discussions. This work was funded by the German State of Lower Saxony and the German Federal Ministry of Economics and Energy (BMWi) within the research project “Upgrade Si-PV” under contract No. 0325877B.

References

[1] Fischer H, Pschunder W. Investigation of Photon and Thermal Induced Changes in Silicon Solar Cells. In: *Proceedings of the 10th IEEE Photovoltaic*. New York: IEEE; 1973, p. 404–11.

[2] Schmidt J, Aberle AG, Hezel R. Investigation of carrier lifetime instabilities in CZ-grown silicon. In: *Proceedings of the 26th IEEE PVSC*; 1997, p. 13–8.

[3] Glunz SW, Rein S, Warta W, Knobloch J, Wettling W. On the degradation of Cz-silicon solar cells. In: *Proceedings of the 2nd World Conference on Photovoltaic Solar Energy Conversion*; 1998, p. 1343–6.

[4] Herguth A, Schubert G, Kaes M, Hahn G. A new approach to prevent the negative impact of the metastable defect in boron doped Cz silicon solar cells. In: *Proceedings of the IEEE 4th World Conference on Photovoltaic Energy Conference*; 2006, p. 910–43.

[5] Herguth A, Schubert G, Kaes M, Hahn G. Investigations on the long time behavior of the metastable boron–oxygen complex in crystalline silicon. *Prog. Photovolt: Res. Appl.* 2008;16:135–40, doi:10.1002/pip.779.

[6] Lim B, Bothe K, Schmidt J. Deactivation of the boron–oxygen recombination center in silicon by illumination at elevated temperature. *phys. stat. sol. (RRL)* 2008;2:93–5, doi:10.1002/pssr.200802009.

[7] Herguth A, Hahn G. Kinetics of the boron-oxygen related defect in theory and experiment. *Journal of Applied Physics* 2010;108:114509-1-7.

[8] Voronkov V, Falster R. Permanent deactivation of boron-oxygen recombination centres in silicon. *Phys. Status Solidi B* 2016:1–8, doi:10.1002/pssb.201600082.
[9] Steckenreiter V, Walter DC, Schmidt J. Kinetics of the permanent deactivation of the boron-oxygen complex in crystalline silicon as a function of illumination intensity. *AIP Advances* 2017;7:35305, doi:10.1063/1.4978266.
[10] Hallam BJ, Hamer PG, Wang S, Song L, Nampalli N, Abbott MD, Chan CE, Lu D, Wenham AM, Mai L, Borojevic N, Li A, Chen D, Kim MY, Azmi A, Wenham S. Advanced Hydrogenation of Dislocation Clusters and Boron-oxygen Defects in Silicon Solar Cells. *Energy Procedia* 2015;77:799–809, doi:10.1016/j.egypro.2015.07.113.
[11] Hamer P, Hallam B, Abbott M, Chan C, Nampalli N, Wenham S. Investigations on accelerated processes for the boron–oxygen defect in p-type Czochralski silicon. *Solar Energy Materials and Solar Cells* 2016;145:440–6, doi:10.1016/j.solmat.2015.11.013.
[12] Hamer P, Nampalli N, Hameiri Z, Kim M, Chen D, Gorman N, Hallam B, Abbott M, Wenham S. Boron-Oxygen Defect Formation Rates and Activity at Elevated Temperatures. *Energy Procedia* 2016;92:791–800, doi:10.1016/j.egypro.2016.07.070.
[13] Wilking S, Ebert S, Herguth A, Hahn G. Influence of hydrogen effusion from hydrogenated silicon nitride layers on the regeneration of boron-oxygen related defects in crystalline silicon. *Journal of Applied Physics* 2013;114:194512, doi:10.1063/1.4833243.
[14] Kern W, Puotinen DA. Cleaning solutions based on hydrogen peroxide for use in silicon semiconductor technology. *RCA Rev.* 1970:187–206.
[15] Schmidt J, Veith B, Brendel R. Effective surface passivation of crystalline silicon using ultrathin Al2O3 films and Al2O3/SiNx stacks. *phys. stat. sol. (RRL)* 2009:287–9, doi:10.1002/pssr.200903272.
[16] Walter DC, Lim B, Bothe K, Voronkov VV, Falster R, Schmidt J. Effect of rapid thermal annealing on recombination centres in boron-doped Czochralski-grown silicon. *Appl. Phys. Lett.* 2014;104:042111-1-042111-4.
[17] Palmer DW, Bothe K, Schmidt J. Kinetics of the electronically stimulated formation of a boron-oxygen complex in crystalline silicon. *Phys. Rev. B* 2007;76, doi:10.1103/PhysRevB.76.035210.
[18] Kane DE, Swanson RM. Measurement of the Emitter Saturation Current by a Contactless Photoconductivity Decay Method. In: *18th PVSC Proceedings*; 1985, p. 578–83.
[19] Bothe K, Schmidt J. Electronically activated boron-oxygen-related recombination centers in crystalline silicon. *J. Appl. Phy. (Journal of Applied Physics)* 2006;99:013701-1-013701-11.
[20] Schulte-Huxel H, Witteck R, Holst H, Vogt MR, Blankemeyer S, Hinken D, Brendemuhl T, Dullweber T, Bothe K, Kontges M, Brendel R. High-Efficiency Modules With Passivated Emitter and Rear Solar Cells—An Analysis of Electrical and Optical Losses. *IEEE J. Photovoltaics* 2017;7:25–31, doi:10.1109/JPHOTOV.2016.2614121.
[21] Hannebauer H, Dullweber T, Baumann U, Falcon T, Brendel R. 21.2%-efficient fineline-printed PERC solar cell with 5 busbar front grid. *Phys. Status Solidi RRL* 2014;9999:n/a, doi:10.1002/pssr.201409190.
[22] Schmidt J, Cuevas A, Rein S, Glunz SW. Impact of light-induced recombination centres on the current-voltage characteristic of czochralski silicon solar cells. *Prog. Photovolt: Res. Appl.* 2001;9:249–55, doi:10.1002/pip.373.